Relation of the plasmapause to the outer radiation belt from DMSP, IMAGE, and SAMPEX observations

W. R. Johnston[1], P. C. Anderson[1], J. Goldstein[2], and S. G. Kanekal[3]

[1]W. B. Hanson Center for Space Sciences, University of Texas at Dallas, Richardson, TX [2]Southwest Research Institute, San Antonio, TX [3]Laboratory for Atmospheric and Space Physics, University of Colorado at Boulder, Boulder, CO

Abstract

The plasmapause separates cold dense plasma in the inner magnetosphere from hot, low density plasmasheet ions. This boundary, typically at 4-6 R_E, tends to show a duskside bulge but is also very dynamic in response to changes in magnetospheric convection and other storm time phenomena. The outer radiation belt is likewise dynamic during stormtime, in terms of both radial location and energetic particle population. It has been proposed that outer radiation belt particles are variously depleted and energized due to wave-particle interactions associated with the plasmapause location. This may be tested by simultaneous observations of energetic particles and the plasmapause location. SAMPEX observations of radiation belt particles may be compared with plasmapause observations from IMAGE, but these provide limited temporal coverage. We will use data from DMSP satellites to identify the plasmapause signature in the ionosphere (specifically the light ion trough) to provide more continuous plasmapause observations. Initial comparisons of DMSP-derived plasmapause locations to IMAGE-based observations as well as outer radiation belt dynamics from SAMPEX show good correlations.

Overview

Plasmasphere-radiation belt interactions

The Earth's plasmasphere is dynamically influenced by magnetospheric and ionospheric electric fields. To first order, it comprises the region where closed corotating field lines contain trapped plasma (Fig. 1). Studies have shown that plasmasphere is highly variable both spatially and temporally, responding to changes in geomagnetic indices, ring current, penetration and shielding electric fields, and subauroral electric fields. Consequently the plasmasphere exhibits erosion, emptying, and refilling during active times, along with a high level of structure. The plasmapause, or outer plasmasphere boundary, is typically located at L=4-6 but may be found at L=2 during active times.

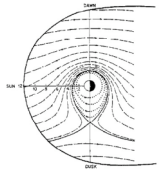

Fig. 1. Convection paths for plasma in magnetosphere, which are along equipotentials of the superposition of the corotation and solar-wind driven electric fields. Within the plasmapause, flux tube motion is dominated by corotation; outside this boundary motion is dominated by convection. Duskside bulge is evident. (From Kavanagh et al., 1968)

The evolution of the plasmapause during active times can significantly affect the outer radiation belt:

• *Summers et al.* (1998) found that enhanced electromagnetic ion cyclotron (EMIC) waves within the plasmasphere tend to scatter trapped electrons into the loss cone, depleting radiation belt particles inside the plasmapause. At the same time, outside the plasmapause whistler-mode waves tend to energize trapped electrons (Fig. 2).

• *Goldstein et al.* (2005) found that the outer radiation belt responded to radial movement of the plasmapause during disturbed times with a time lag of several days.

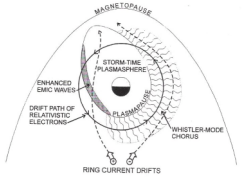

Fig. 2. Schematic of proposed mechanism for outer radiation belt energization and loss associated with the plasmasphere. (From *Summers et al.*, 1998.)

Plasmapause-ionosphere interactions

Several ionospheric signatures of the plasmapause have been proposed, including:

• midlatitute electron density trough
• total electron content (TEC)
• subauroral electron temperature enhancement (SETE)
• precipitating electron boundary
• stable auroral red arcs (SARS)
• light ion trough (LIT)

There is generally not a one-to-one correspondence between any of these and the plasmapause. Regarding LIT:

• *Taylor and Walsh* (1972) found it one of the more consistent signatures, whereas

• *Foster et al.* (1978) found the LIT generally a few degrees equatorward of the plasmapause as identified by whistler waves.

Satellites/instrumentation: DMSP, IMAGE, SAMPEX

DMSP: polar sun-synchronous orbits, alt. 840 km, period 100 min., generally 3-4 operational at any given time. During 2001 data is available from F12, F14, and F15 in pre-midnight to morning and F13 in dusk to dawn. Instruments include:

• Retarding Potential Analyzer (RPA) providing ion density and composition
• Ion Drift Meter (IDM)
• Precipitating Electron and Ion Detectors (SSJ/4)

IMAGE: eccentric polar orbit (from 1400 km alt. to 8 R_E), operational 3/2000 to 12/2005. Instruments include:

• EUV imagers directly imaging 30.4 nm UV scattered by plasmaspheric He^+. Such imaging is feasible when IMAGE is near apogee (Fig. 3).

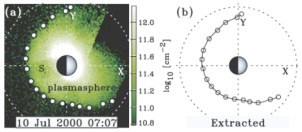

Fig. 3. Sample IMAGE EUV image of plasmasphere, showing extracted plasmapause locations. (From *Goldstein et al.*, 2004)

SAMPEX: low Earth orbit, alt. from 500 km to 620 km in 2001, operational 7/1992, includes four instruments for energetic particle measurements:

• Heavy Ion Large Area Proportional Counter Telescope (HILT)
• Low Energy Ion Composition Analyzer (LEICA)
• Mass Spectrometer Telescope (MAST)
• Proton/Electron Telescope (PET)

Methodology: DMSP-derived plasmapause locations

Choosing the LIT to identify the plasmapause, we used DMSP data to identify the high-latitude gradient in H^+ density. From a log-linear fit to this section of data, we have initially used a density threshold of 10^3 cm^{-3} as the plasmapause boundary.

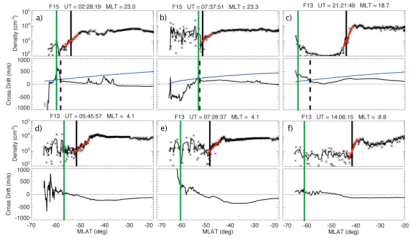

Fig. 4 shows sample DMSP observations for evening-side (a-c) and morning-side passes (d-f), in each case showing H^+ density (top) and ion cross-drift velocity (bottom):

• vertical green line--electron precipitation boundary
• red line--log-linear fit to density data
• solid black vertical line--derived plasmapause locations, i.e. where linear fit crosses adopted threshold of 10^3 cm^{-3}

Evening-side passes also show:

• blue line--negative of corotation drift
• dashed vertical line--convection stagnation point

The sequence 4a-4c shows plasmasphere evolution through a storm:

a) stagnation boundary slightly poleward of plasmapause boundary: plasmasphere still refilling after previous depletion;

b) stagnation boundary has moved due to stormtime penetration E fields, subauroral E fields nearly to plasmapause boundary;

c) during storm recovery E field and stagnation boundary return to high latitudes, leaving eroded plasmasphere with sharp boundary to begin refilling.

Morning-side passes 4d-4f also show erosion, plasmapause boundaries but no stagnation boundary (convection, corotation in same direction)

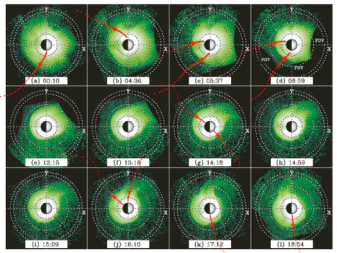

Fig. 5 shows IMAGE EUV observations of He^+ plasmapause on 18 July 2001 projected to SM X-Y plane (from *Goldstein and Sandel*, 2005). Sun is to right, dusk at top. Red traces show DMSP F13 and F15 orbit tracks mapped to X-Y plane in SM coordinates using the IGRF 2000 and Tsyganenko 2001 magnetic field models. Red crosses indicate location of ionospheric projection of plasmapause derived from the DMSP H^+ observations as described above.

Case study: comparison with IMAGE, SAMPEX

Dynamic behavior of the plasmapause and radiation belt in early 2001 was studied by *Goldstein et al.* (2005). Initially we applied our DMSP-based approach to this period, permitting comparison of DMSP- and IMAGE-derived plasmapause locations.

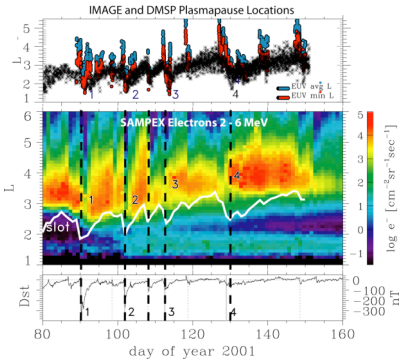

Fig. 6 shows these results superimposed on IMAGE/SAMPEX data (from *Goldstein et al.*, 2005):

• Top frame shows IMAGE-derived plasmapause locations from each EUV image (red, average L; blue, minimum L) and all DMSP-derived plasmapause locations (black), which complement gaps in IMAGE coverage.

• Second frame shows SAMPEX electron counts (2-6 MeV) as daily averages, with the daily average DMSP-derived plasmapause location shown as white line. The inner edge of the outer radiation belt moves inward a few days after inward motion of plasmapause during disturbances 1 and 2--but not following inward motion of plasmapause during disturbance 4.

• Third frame shows Dst index. Note correlation between DMSP-derived plasmapause locations and Dst, including several intermediate disturbances.

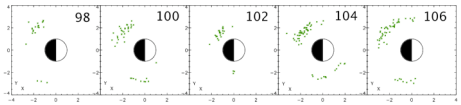

Fig. 7 shows derived plasmapause locations for five days mapped to SM X-Y plane using the IGRF 2000 and Tsyganenko 2001 magnetic field models. Each plot shows all identified locations for the day number indicated. Sun is to right, dusk at top. The sequence spans disturbance 2:

• days 98, 100--pre-disturbance, quiet with a filled plasmasphere;
• day 102--peak plasmasphere erosion in middle of disturbance;
• days 104, 106--gradual plasmasphere refilling.

Conclusions and future work

Initial results from the case study for early 2001 show

• Plasmapause locations from DMSP correlate well with those from IMAGE;
• Outer radiation belt location found by SAMPEX generally responds to changes in plasmapause location with a delay of several days--this holds for most disturbances, but not for disturbance 4 on 30 May; and
• DMSP-derived plasmapause location correlates well with Dst for disturbances of varying intensities.

The extent of DMSP time coverage will permit comparisons to SAMPEX, including the period from 1996 to 1998 when SAMPEX spacecraft rotation permitted derivation of pitch angle information. These data will be used to examine the relationship of the plasmasphere and radiation belt energization and loss.

References

• Foster, J. C., et al. (1978), *JGR* 83:1175-1182.
• Goldstein, J., et al. (2004), *GRL* 31:L01801.
• Goldstein, J., S. G. Kanekal, D. N. Baker, B. R. Sandel (2005), *GRL* 32:L15104.
• Goldstein, J., and B. R. Sandel (2005), in *Inner Magnetosphere Interactions*, doi:10.1029/2004BK000104.
• Kavanagh, L. D., Jr., et al. (1968), *JGR* 73:5511-5519.
• Summers, D., R. M. Thorne, F. Xiao (1998), *JGR* 103(A9):20487-20500.
• Taylor, H. A., Jr., and W. J. Walsh (1972), *JGR* 77:6716-6723.